6.1 Introduction

Glutathione (GSH), a thiol-containing tripeptide (Glu-Cys-Gly) is most abundant intracellular non-proteine thiol present in plants, mammals, fungi and some prokaryotes. This thiolated tripeptide present in tissues exist in both the reduced form (GSH) and oxidized dimeric form (GSSH) which led it to maintain the intracellular reduction-oxidation potential. Apart from this, GSH plays a crucial biological role in cellular defence against xenobiotics and free radicals, signal transduction, gene regulation (Lu 2009, Chen *et al*. 2012, Estrela *et al*. 2006). Hence, because of its important biological role, it is an urgent need to develop a novel and efficient technique to monitor the changes in concentration of GSH in biological fluids.

Nano-biotechnology is an emerging field of science and technology for the development, improvement and utility of nanostructures. Since last two decades, the green synthesis of gold nanoparticles (AuNPs) has received a considerable attention of the researchers due to growing need in various fields; such as, catalysis (Shen *et al*. 2017), biosensing (Varun *et al*. 2017), biological (Hoshyar *et al*. 2016), electronics, photonics, drug delivery, biolebelling (Daniel and Astruc 2004), wound dressings (Yang *et al*. 2017) and medicine (Ribeiro *et al*. 2017). The concentration of GSH ranged from milli molar (cells of tissues and organs) to micromolar (plasma, saliva, cerebrospinal fluid, urine) which changes dramatically under oxidative stress (Pastore *et al*. 2003). The imbalance of cellular GSH lead to several diseases, such as aging, cancer, liver damage, luecocytes loss, psoriasis, liver damage heart problems and others (Townsend *et al*. 2003, Shi *et al*. 2014, Shamsipur *et al*. 2014, Gupta *et al*. 2016). At present, plant extracts mediated green synthesis of AuNPs has proven to be more advantageous over other biological systems because it does not require the

aseptic conditions, and maintenance of microbial culture (Kumar *et al*. 2017a, Anand *et al*. 2015). In addition to this, the plant extract mediated synthesis is user-friendly economically efficient and environment-friendly (Kumar *et al*. 2017b). The plant extract are reported to contain several phytochemicals such as tannins, flavonoids, terpenoids, proteins, hydrogenases, and reductases etc. which are responsible for both reduction and stabilization of AuNPs (Kumar *et al*. 2017a). Hence, currently the plant extracts are being used extensively as a reducing and stabilizing agent for the synthesis of AuNPs. Recently, several plants like *Pogestemon benghalensis* (Paul *et al*. 2015), *Avera lanata* (Joseph and Mathew 2015), *Stevia reboundiana* (Sadeghi *et al*. 2015), *Eucalyptus oleosa* (Pourmortazavi *et al*. 2017) have been used for the synthesis of AuNPs.

The photoinduced green synthesis of AuNPs using plant extract is proved to be more economic efficient and eco-friendly where the rate of biosynthesis is increased by visible light (Kumar *et al*. 2016a). There are several articles which have been published for the biosynthesis of AuNPs using sunlight induced route. In our previous study we have reported the photoinduced synthesis of AuNPs using aqueous extract of *Croton bonplandianum* (Kumar *et al*. 2017a), *Erigeron bonariensis* (Kumar *et al*. 2016b) *Xanthium strumarium* (Kumar *et al*. 2017b, Kumar *et al*. 2016c) and *Murraya koenigi* (Kumar *et al*. 2017b) and *Physalis angulata* (Kumar *et al*. 2017c) through sunlight induced route.

The plant *Croton bonplandianum*, (Three-Leaved Caper) is a native weed to the Southern Bolivia, Paraguay, Southwestern Brazil and Northern Argentina. It belongs to family Euphorbiaceae and commonly found in India as an exotic weed along the roads, canal and other water-stressed area. In spite of having medicinal value, it has a great composition of

reducing as well as capping agent required for the potent biosynthesis of AuNPs (Reddy 1988, Vadlapudi 2010).

The main aim of the current investigation is to apply the principles of green chemistry for the development of a green, simple and eco-friendly route for the synthesis of stable AuNPs by optimizing several process parameters using one parameter at a time approach. In addition to this, it was aimed at not to use any hazardous chemical, sophisticated instrumentation, heating and stirring too throughout the synthesis of AuNPs. The investigation of effect of different metal ion concentrations on the shape and size of AuNPs and crystallinity was one of important part of our aim. Finally, the optimum AuNPs thus obtained was investigated for its peroxidase-like activity towards the oxidation of TMB with the development of blue color which was considered as a base for the detection of GSH.

6.2 Materials and methods

6.2.1 Preparation of leaf extract

The preparation of leaf extract is discussed in chapter 4 section 4.2.1

6.2.2 Biosynthesis of AuNPs

In order to investigate the effectiveness of photocatalytic activity of sunlight, the biosynthesis reaction of AuNPs was carried out both in natural sunlight and dark condition. The temperature of the ambient environment in sunlight and solar intensity of incident sunlight radiation were 39 °C and 66300 lux respectively. The temperature of the dark condition and light intensity were 32°C and 0 lux respectively. To avoid the fluctuation in temperature and sunlight intensity, the synthesis reactions were carried out between 12 pm to

2 pm. For the synthesis purpose, 2% (v/v) of AEC inoculum dose was added into 2 mL of 0.8 mM $HAuCl_4.xH_2O$ solution at neutral pH and kept in both bright sunlight and dark condition.

Therefore, further all the AuNPs synthesis experiments were performed in bright sunlight for the optimization of the other process parameters using one factor at a time approach. The process parameters such as sunlight exposure time, AEC inoculum dose and $HAuCl_4.xH_2O$ concentration were screened for optimization purpose in the range from 0 min to 24 min, 1.0% to 8.0% (v/v), and from 0.4 mM to 3.2 mM respectively. After the optimization of reaction at these conditions, the synthesized AuNPs were purified by centrifuging at 15000 rpm for 15 min and subsequently re-dispersing in UPW to remove the water soluble molecules and other secondary metabolites. The final mass of AuNPs was collected by vacuum drying after repeating this process four times.

6.2.3 Experimental methodology

The AuNPs thus obtained were characterized through various instrumental techniques empowering the nanotechnology. The primary confirmation of AuNPs was studied using UV–Visible spectrophotometer (Evolution 201, Thermo Scientific) in the range of 300 to 800 nm. Fourier Transform Infrared Spectrophotometer (FTIR, Perkin Elmer Spectrum 100) was used to study the involvement of various functional groups in the range of 4000–400 cm^{-1}. The crystallinity of AuNPs was investigated using X-ray Diffractometer (Rigaku Miniflex II) having Cu Kα radiation source and Ni filter in the range of 20° to 80° at scanning rate of 6° min^{-1} with a step size 0.02°. The morphology and size of the biosynthesized AuNPs was further confirmed by Transmission Electron Microscopy (TEM) carried out on TECNAI 20 G2-electron microscope operated at accelerating voltage 200 kV. Zeta-potential of the AuNPs was measured using a Malvern Zetasizer (Malvern Instruments, Ltd.). The elemental

composition and purity of powdered sample was confirmed by EDX analysis equipped with TEM. The Selected Area Electron Diffraction (SAED) demonstrated the concentric diffraction rings which also confirmed the crystalinity of synthesized AuNPs. The speciation of biosynthesized AuNPs was confirmed by X-Ray Photoelectron Spectroscopy (XPS, AMICUS, Kratos Analytical, A Shimadzu) with Mg Kα (1253.6 eV) radiation as X-ray source. Thus obtained AuNPs showed peroxidase-like mimetic which was applied in the colorimetric detection of glutathione and given in detail in chapter 2 under section 2.5

6.3 Results and discussion

6.3.1 Primary confirmation of AuNPs synthesis

The surface plasmon resonance (SPR) produced through collective oscillations of free conduction electrons caused to change in color of the reaction mixture from yellowish to purple. This change in color was the primary confirmation of biosynthesis of AuNPs. The reaction mixture exposed to bright sunlight exhibited the development of dark purple color and sharp SPR band within 16 min of AEC inoculation into $HAuCl_4.xH_2O$ solution which showed the rapid synthesis of AuNPs whereas the reaction mixture kept at dark condition failed to attain the characteristics brown color even after 10 hrs of incubation **(Fig. 6.1)**. This time lag clearly indicated that the potent biosynthesis of AuNPs was much faster in bright sunlight as compared to darker condition. The UV–visible absorption spectroscopy is a novel tool to examine the formation AuNPs. The effect of bright sunlight exposure on the synthesis of AuNPs, color change and the pattern of SPR band was studied by withdrawing the samples from reaction mixture at regular time interval of 4 min and screened between 300 to 800 nm through UV-visible spectroscopy.

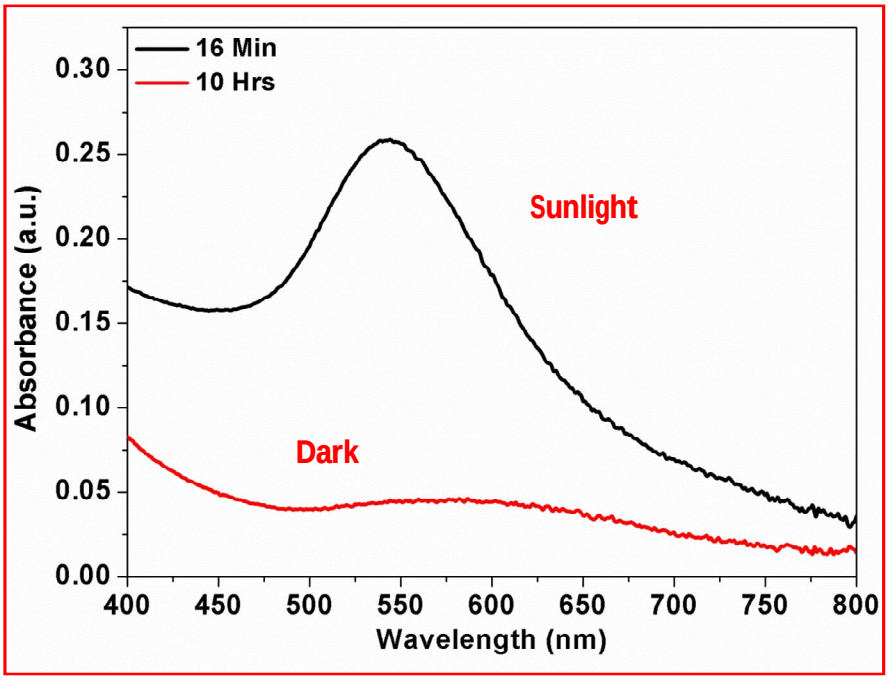

Figure 6.1 UV-visible spectra of AuNPs synthesis in sunlight and dark condition with inset photograph of respective color change

It was found that after 24 min of bright sunlight exposure, the screened samples showed a SPR band at 542 nm which attributed to the characteristic surface plasmon resonance of AuNPs having λ_{max} values in the range of 500-600 nm (Reddy *et al*. 2012).

6.3.2 Optimization of the process parameters

6.3.2.1 Sunlight exposure

The optimization of sunlight exposure time for the synthesis of AuNPs was carried out by screening the reaction mixtures at each 4 min of interval. It was noticed that as the exposure time increased, the pattern of changing color from light yellow to dark purple of each AEC doses increased (**Fig. 6.2A-H**). The intensity and color of the reaction mixture of

first 8 min and 4 min of exposure of 1% and 2% AEC respectively did not show characteristics SPR band and change in color due to the absence of the nuclei with the radius

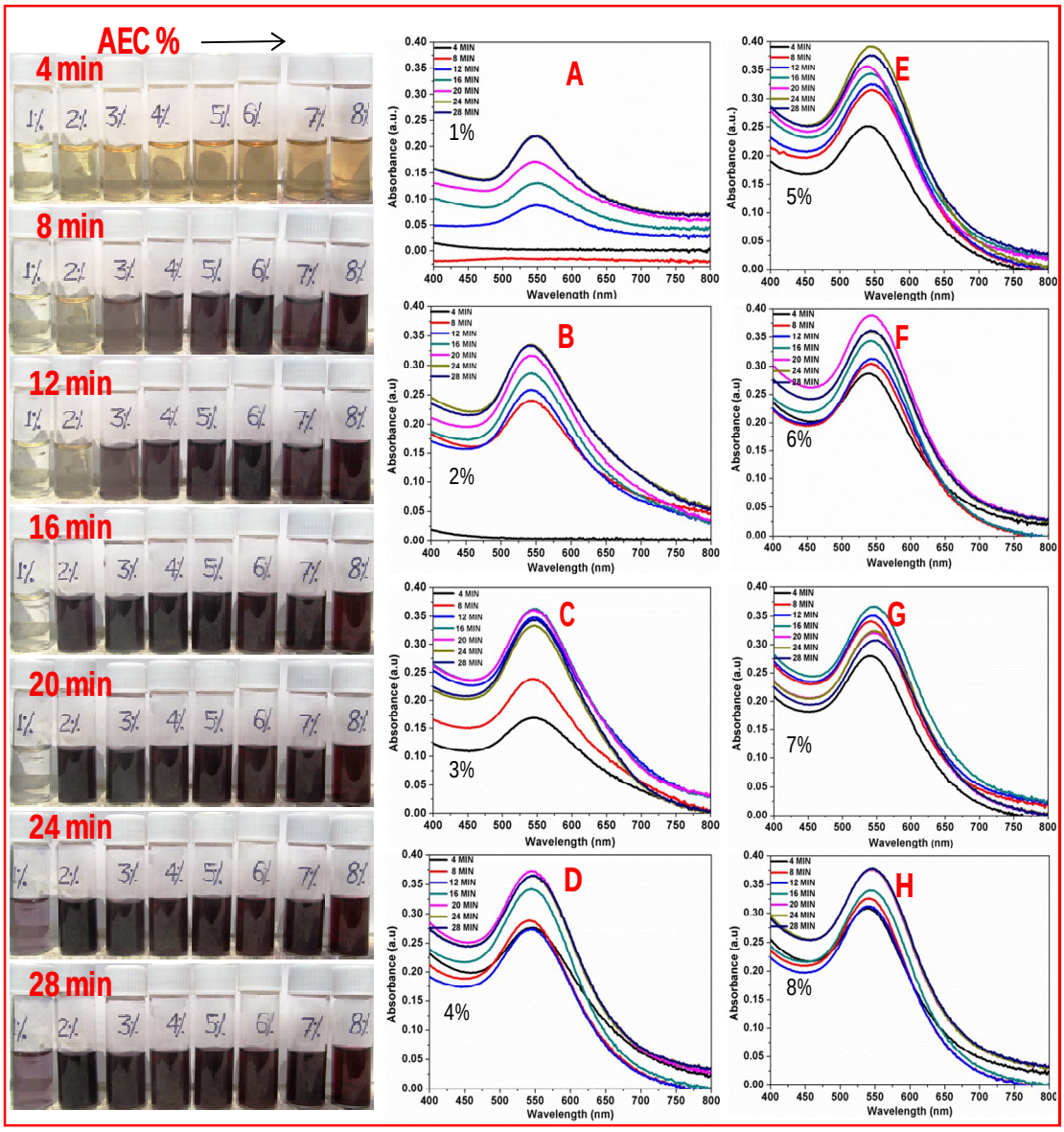

Figure 6.2 UV–visible absorption spectra of AuNPs synthesis using different AEC inoculums doses from 1% to 8% (A – H respectively) and their corresponding increase in intensity and color change pattern with the proceeding of time from 4 to 28 min (conditions; 0.8 mM $HAuCl_4.xH_2O$ concentration and 4 to 28 min sunlight exposure time and 1% to 8% AEC inoculums dose)

larger than critical radius which re-dissolved in the reaction mixture and failed to nucleate to form AuNPs (**Fig. 6.2A and B**) (Peng and Yang 2009, Bøjesen and Iversen 2016). Thereafter, the intensity of the SPR band continued to be increased up to 24 min of each inoculums dose by 4% AEC and after that no significant increase in SPR band intensity was observed ((**Fig. 6.2A-D**). The increase in intensity signified the increased synthesis of AuNPs whereas further no increase in SPR band intensity corroborated the establishment of the equilibrium (Kumar *et al*. 2017c). Thereafter, an interesting result was obtained while screening the SPR band pattern of 5% to 8% AEC (Kumar *et al*. 2017b). A regular pattern of decreasing of SPR band intensity was observed with the increase in AEC doses from 5% to 8% after achieving the maximum intensity with the proceeding of exposure time. This interesting pattern was due to the increased agglomeration and accordingly decreased SPR band intensity with the time by increasing AEC doses (**Fig. 6.2E-H**).

6.3.2.2 AEC inoculums dose

Figure 6.2A-H represented the UV-visible spectra of AuNPs produced by different stock solution of AEC from 1.0% to 8.0%. While screening it was observed that as the AEC dose increased from 1% to 8%, the color intensity of the reaction mixture increased from light purple to dark purple at each time interval which indicated the increased synthesis of AuNPs (Kumar *et al*. 2016c). The pattern of UV-visible spectra revealed that with the increase in stock solution, the intensity of the SPR band increased upto 4%. Thereafter, a decreasing pattern of SPR band was observed after each 4 min of exposure time. It was noticed that the exposure time required for the development of the SPR band and the color of the solution decreased with the increasing amount of the AEC stock solution (**Fig. 6.2A-H).** When 1% AEC was screened, a single SPR was produced with broader and less intense peak

having large FWHM which suggested that the synthesized AuNPs were fewer in number. Further, on increasing the AEC dose up to 4.0 %, the intensity of the SPR band increased up to 24 min exposure time which indicated the increased synthesis of AuNPs with increasing the AEC dose (Kumar *et al*. 2017a). Thereafter, by using 5%, 6%, 7% and 8% AEC, a gradual decrease in SPR band intensity was observed. The decreasing of the sharpness and increase in broadening of the SPR band towards longer wavelength was due to the overgrowth of the AuNPs which got lighter in color due to settling at the bottom that can be seen very clearly from the attached vial color of 8% AEC after 28 min exposure time. Therefore 4% AEC was considered as optimum for the synthesis of AuNPs.

6.3.2.3 $HAuCl_4.xH_2O$ concentration

The synthesis of AuNPs was also optimized using varying concentration of $HAuCl_4.xH_2O$ from 0.4 mM to 3.2 mM at 4% AEC stock solution and 24 min of sunlight exposure time. The SPR bands of 0.4 mM, 0.8 mM, 1.2 mM, 1.6 mM, 2.0 mM, 2.4 mM, 2.8 mM and 3.2 mM $HAuCl_4.xH_2O$ concentrations revealed the maximum absorbance at 560 nm, 556 nm, 550 nm, 552 nm, 545 nm and 543 nm, 546 nm and 595 nm respectively after 24 min of sunlight exposure which are shown in **Figure 6.3A-H.** The figures clearly indicated that as the concentration of each $HAuCl_4.xH_2O$ from 0.4 mM to 3.2 mM increased, the color of reaction mixtures darkened gradually from 4 to 24 min. It is well known that the color of AuNPs solution is associated with the size of nanoparticles which was confirmed by TEM analysis. It that the average size of the AuNPs increased from 5.6 nm to 19.4 nm with the increase $HAuCl_4.xH_2O$ concentration from 0.4 mM to 3.2 mM (**Fig. 6.6A-H**). Thus it is clear that the color governs the particle size distribution (Bastus *et al*. 2014). When the

concentrations of $HAuCl_4.xH_2O$ were increased from 0.4 mM to 3.2 mM, a distinct pattern of SPR bands were observed.

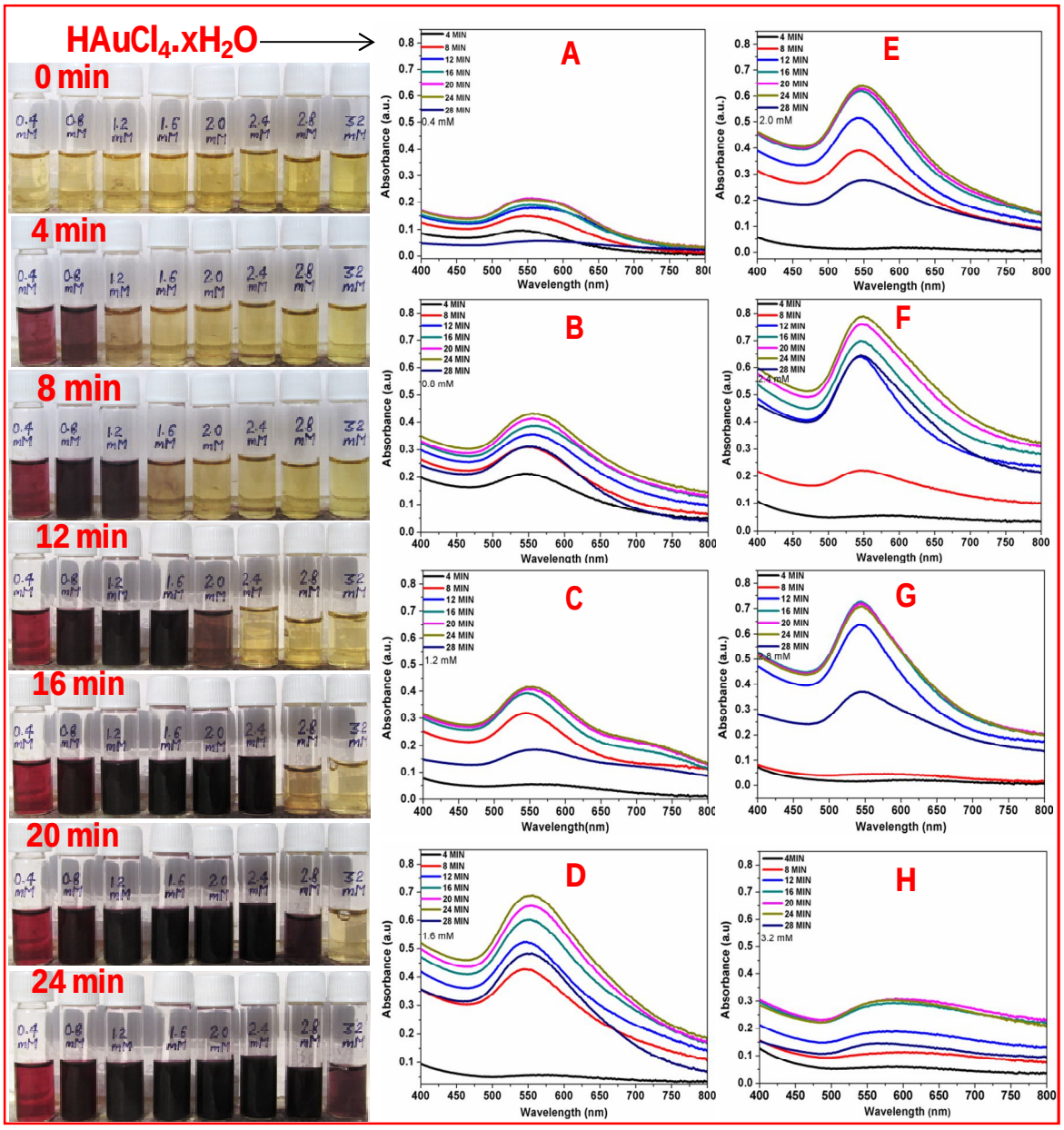

Figure 6.3 UV–visible absorption spectra of AuNPs synthesis using different concentrations of HAuCl4.xH2O from 0.4 mM to 3.2 mM (A – H respectively) using 3% AEC inoculums dose and color change pattern with the proceeding of time from 4 to 24 min (conditions; 3% AEC inoculums dose and 4 to 24 min sunlight exposure time and 0.4 mM to 3.2 mM $HAuCl_4.xH_2O$ concentration)

It was observed that while using 0.4 mM $HAuCl_4.xH_2O$ concentration, the SPR bands obtained were less intense and the color of the solution was also very light which continued to be increase at each time interval from 4-24 min. This indicated the synthesis of very few numbers of AuNPs with smaller size which was also confirmed by the produced TEM image (**Fig. 6.6A**). This pattern of increasing SPR band intensity with time was continued upto 1.6 mM $HAuCl_4.xH_2O$ concentration. The increase in SPR band intensity upto 1.6 mM at each screening time interval indicated that as $HAuCl_4.xH_2O$ concentration increased, the synthesis of AuNPs also increased with increased average size which was further confirmed by TEM images (**Fig. 6.6B-D**) (Lee *et al*. 2016). But when the $HAuCl_4.xH_2O$ concentration increased beyond 1.6 mM, the SPR band produced were broader and steeper towards longer wavelength with continued decreasing intensity upto 3.2 mM. This indicated synthesis of larger AuNPs which might be due to overgrowth as can be seen from the TEM images (**Figure 6.6 E-H**). It is well reported fact that spherical/pseudospherical nanoparticles are formed when the generated nuclei having low concentration of precursor monomers. However, the anisotropic nanoparticles are formed when the generated nuclei having high concentration of precursor monomers. It was observed that on increasing the $HAuCl_3.xH_2O$ concentration, the formation of anisotropic AuNPs like trigonal, rod, hexagonal, pentagonal shaped increased due to increased monomer concentration which is clearly obvious from the results shown in **Figure 6.6 E-H** (Thanh *et al*. 2014).

Therefore, in order to get smaller and large number of AuNPs with controlled growth and smaller size, 1.6 mM $HAuCl_4.xH_2O$ concentration at 4.0% AEC and 24 min exposure time was chosen as optimal condition for the current study.

6.4 Mechanism involving AuNPs formation

Several authors have already reported the presence of polyphenolic compounds (tannin, flavonoids) resins, sugars, proteins, alkaloids, glycosides and steroids through the phytochemical analysis of *C. bonplanadianum* leaf extract (Jeeshna *et al*. 2011). Tannins, flavonoids and sugars act as an effective reducing agent whereas proteins and some other phytochemicals act as stabilizing agent during synthesis of AuNPs (Kumar *et al*. 2016a). The previous phytochemical studies of *C. bonplanadianum*, our ferric chloride test and Folin Ciocalteu's method, photoinduced synthesis of AuNPs and FTIR analysis of AEC, TA, pre-annealed AuNPs and post-annealed AuNPs encouraged us to propose a mechanism of AuNPs synthesis through AEC. The presence of vast variety of phytochemicals in the AEC may follow different reduction routes of Au^{3+} but the presence of tannins (polyphenol) in AEC was comparatively higher than other chemicals. Therefore, the reduction of Au^{3+} was proposed using tannin as a reducing agent.

We have proposed a stepwise mechanism of AuNPs synthesis. When the AEC was added into the $HAuCl_4.xH_2O$ solution, the OH group of polyphenolic compound (tannin) present in AEC bound with Au^{3+} and formed the Au^{3+}/AEC complex. Since, the results clearly showed that the biosynthesis of AuNPs was driven by the photocatalytic effect of sunlight. The first step involved the photoactivation of Au^{3+}/AEC complex where the OH group of AEC produced hydrated electrons by debonding of OH group after absorbing the photons of light, putting strong evidence after the sunlight induced synthesis of AuNPs (Zhou *et al*. 2014, Yang *et al*. 2015). The second step involved the reduction of Au^{3+} to Au^0 by the hydrated electrons produced earlier (Sakamoto *et al*. 2009). The concentration of gold atoms (Au^0) continued to increase with the continued reduction of $HAuCl_4.xH_2O$. When the

increased concentration of Au^0 atoms exceeded the critical supersaturation, the gold atoms started to nucleate and formed the crystal nuclei (**step III**). The formation of these crystal nuclei led to the decrease in concentration of Au^0 atoms below to the critical supersaturation where the whole process is dominated by the growth of nuclei to form nanoclusters because of no longer increase in number of crystal nuclei (**step IV**).

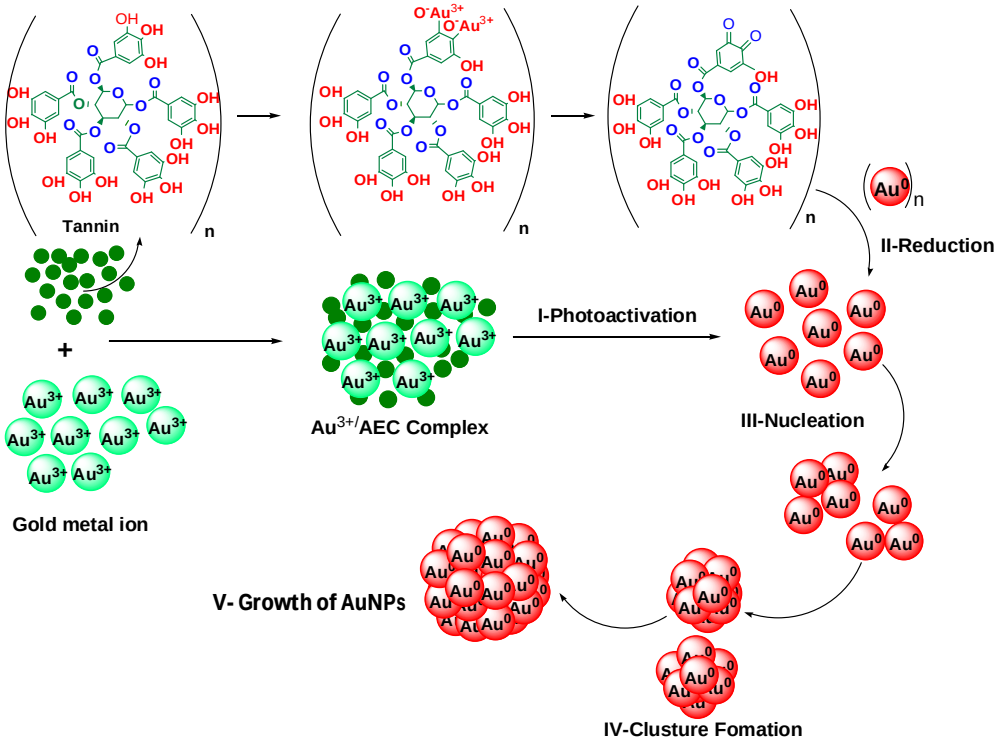

Scheme 6.1 The scheme showing the various steps of AuNPs synthesis by involving the enol form of 'n' number of polyphenolic groups of 'n' number of tannin present in AEC which formed complex (AEC/Au^{3+}) with Au^{3+} and further reduced the n[Au^{3+}] to n[Au^0] by the hydrated electrons released from the debonding of O-H bond. The n[Au^0] formed AuNPs after simultaneous nucleation, cluster formation and further growth

The growth of the nanoclusters further decreased the concentration of Au^0 atoms below the saturation level which stopped the growth of nanoclusters and finally aggregated to form AuNPs (**step V**) (Tran and Nguyen 2011) (**Scheme 1.3**). The photoresponsive nature of

the polyphenolics, and other flavin binding protein present in AEC further advocated to the photocatalytic action of sunlight where the electrons could be easily donated by the polyphenolics in the presence of sunlight or can stimulate other phytochemicals to do the same (Gade *et al*. 2014). In this case proteins, sugars or some other phytochemicals act as stabilizers for AuNPs. The FTIR also advocated to the above fact by illustrating the contribution of –OH and $–NH_2$ groups in synthesis and stabilization of AuNPs. **Scheme 6.1** showed the photoactivation of Au^{3+}/AEC complex (**step I**), reduction of Au^{3+} to Au^0 by involving n(OH) of n(tannin) present in AEC (**step II**), nucleation (**step III**), to form nanocluster (**step IV**) and finally AuNPs by overgrowth (**step V**).

6.5 Characterization

Thus synthesized optimum AuNPs at 24 min of sun light exposure time, 1.6 mM $HAuCl_4.xH_2O$ concentration and 4.0% of AEC stock solution dose was investigated through various modern characterizing techniques such as FTIR, XRD, TEM, SAED, EDX, and XPS analysis.

The identity of the phytochemicals responsible for the biosynthesis and stabilization of AuNPs was explored by FTIR study. On the basis of the phytochemical profile of the leaf extract (given in chapter 2 in section 2.3.2) it was concluded that the polyphenolic compounds like tannin was the main constituents of the AEC. To strengthen this fact, the FTIR analysis of the pure TA was also carried out and matched with the FTIR analysis of the AEC. **Figure 6.4** represented the FTIR spectra of pure TA, AEC, pre-annealed AuNPs and post-annealed AuNPs. The FTIR spectrum of pure TA was well matched with the FTIR spectra of AEC to confirm the presence of specific functional groups of tannin present in AEC. The FTIR spectrum of AEC was taken as a control and compared with the FTIR

spectra of pre-annealed AuNPs to identify major functional groups responsible for the biosynthesis of the AuNPs. The phytochemicals involved in the capping of the AuNPs was also confirmed by comparing the FTIR analysis of post-annealed AuNPs with the FTIR analysis of pre-annealed AuNPs. It was found that the FTIR spectrum of the pure (tannic acid) TA showed the characteristics band at 3339 cm^{-1} (υ_s of OH), 2939 cm^{-1} (υ_s of C=C-H), 1711 cm^{-1} (υ_s of CO), 1616 cm^{-1} (υ_s of C=C), 1449 cm^{-1} (υ_s of C=C), 1340 cm^{-1} (υ_s of C=C) 1020 cm^{-1}(υ_s of O-C) and 620 cm^{-1}(υ_b, bending vibration) (Kumar *et al*. 2017a). When the FTIR spectrum of the AEC was carried out, it was noticed that it showed the similar band as shown by TA.

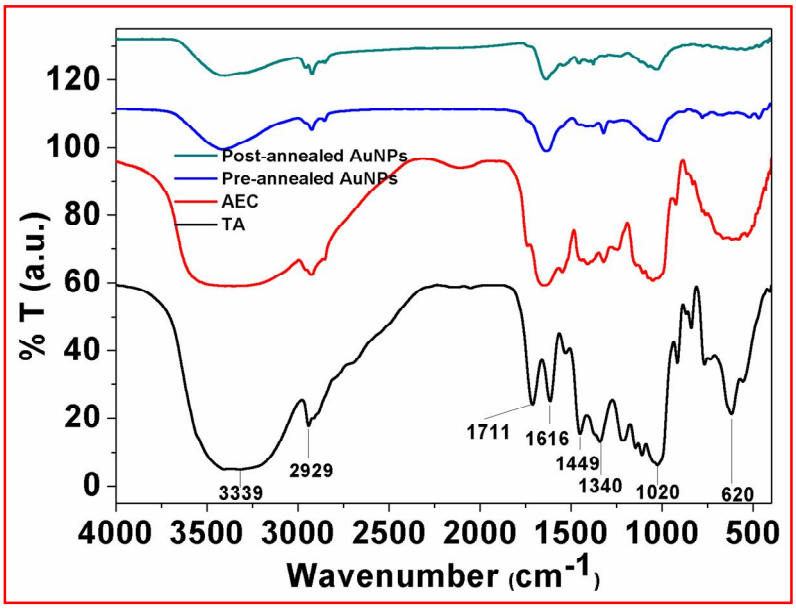

Figure 6.4 FTIR spectra of pure TA, AEC, pre-annealed and post-annealed AuNPs showing the involvement of various functional groups for the synthesis and stabilization of AuNPs

The presence of similar characteristics band both in TA and in AEC confirmed the presence of tannin like moieties (polyphenolic). The presence of tannin in AEC was also strengthened by carrying out an experiment which instantly turned the greenish yellow color of the AEC to dark green color after adding 0.1% of $FeCl_3$ solution (Dutta and Ray 2014). The FTIR spectrum of the pre-annealed AuNPs revealed the same characteristic bands as that of AEC except some diminishing and shifting which advocated the important role of phytochemicals present in AEC involved in the synthesis and capping of the AuNPs. Both the spectra showed a shifting in following peaks: from 3359 to 3415 cm^{-1} (band due to υ_s of OH of the polyphenolic compounds and υ_s of NH of the proteins), 1051 cm^{-1} to 1027 cm^{-1} (υ_s of O-C) (Huang *et al*. 2010, Nakano *et al*. 2001). The peak present at 2929 cm^{-1} (υ_s of C=C-H), 1640 cm^{-1} (υ_s of C=C), and 1318 cm^{-1} (υ_s of C=C) did not show any shift rather diminishing whereas the peak present at 610 cm^{-1} completely disappeared. These investigations revealed the important role played in the biosynthesis of AuNPs by the hydroxyl, carboxyl, amino and amide groups of phytochemicals present in AEC. The tannins, glucose and protein present in AEC could be the major source of these groups. The FTIR spectra of post-annealed AuNPs showed diminishing in the intensity of the characteristics peak which confirmed the loss of phytochemicals involved in the capping of AuNPs.

The crystalline nature of the AEC synthesized AuNPs of all the metal ion concentrations (0.4 to 3.2 mM) was determined by XRD analysis. The data were collected in the angular range $30° \leq 2\theta \leq 80°$ with step size 0.02° and scan rate 6° min^{-1}.The characteristic XRD patterns of AuNPs are represented in **Figure 6.5** with the diffraction peaks observed at $2\theta = 38.06^{\circ}$, 44.24°, 64.47° and 77.3°.

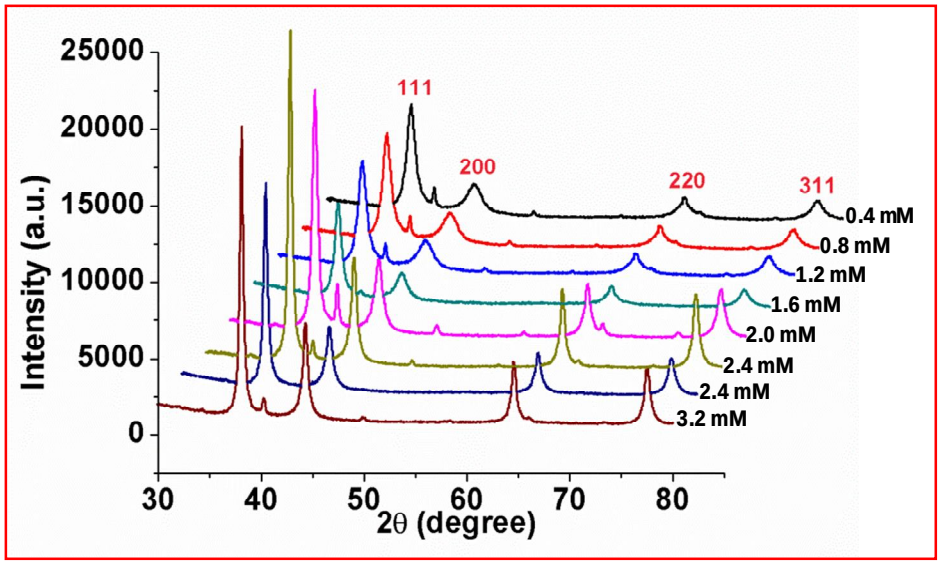

Figure 6.5 X-ray diffraction patterns of AuNPs obtained from different $HAuCl_4.xH_2O$ concentration (0.4 mM to 3.2 mM)

Table 6.1 Comparison table showing the average size obtained from TEM and XRD analysis

S.N.		TEM	XRD
	Metal ion concentration (mM)	Average Size (nm)	Average size (nm)
1	0.4	5.6	7.1
2	0.8	5.7	7.4
3	1.2	6.1	9.3
4	1.6	8.6	10.4
5	2.0	13.2	13.4
6	2.4	14.5	16.4
7	2.8	17.7	20.3
8	3.2	19.4	22.2

The peaks of AuNPs synthesized from 0.4 to 3.2 mM were well matched with standard diffraction data with those reported for gold by Joint Committee on Powder Diffraction Standards (JCPDS) file no: 040784 and attributed to (111), (200), (220) and (311) Bragg reflections respectively. These Bragg reflections corresponded to the crystalline planes of the face centered cubic (fcc) crystal lattice of metallic gold. The average estimated crystallite size of the all the metal ion concentrations (0.4 to 3.2 mM) AuNPs were consistent with the average sizes of AuNPs obtained from the HR-TEM analysis (**Table 6.1**).

The exact size and morphology of the AuNPs was analyzed using different concentration of $HAuCl_4.xH_2O$ (0.4 mM to 3.2 mM) and was investigated through HR-TEM analysis. For the HR-TEM analysis, AuNPs suspension obtained from all the $HAuCl_4.xH_2O$ (0.4 mM to 3.2 mM) concentrations were first diluted by UPW (1:3). Further, the carbon coated copper grids were dipped into respective AuNPs solutions and then dried under table lamp for two hr and loaded onto a specimen holder. The HR-TEM images of AuNPs with different magnifications produced from 0.4 mM to 3.2 mM are shown in **Figure 6.6A-H.** The HR-TEM images obtained from 0.4 mM revealed the presence of smaller and spherical AuNPs. The images at different magnification also revealed that there were very less number of particles distributed throughout the mass of the samples which was in accordance with the change in color and SPR band intensity. The corresponding size distribution histogram of AuNPs represented that maximum AuNPs were in range of 2.5 nm to 4.5 nm having average size distribution of 5.6 nm. Whereas when the concentration of the $HAuCl_4.xH_2O$ increased to 0.8 mM, the number of spherical shaped AuNPs increased. The corresponding size distribution histogram represented that the synthesized AuNPs were in the range of 1.4 nm to 11.8 nm with the average size 5.7 nm.

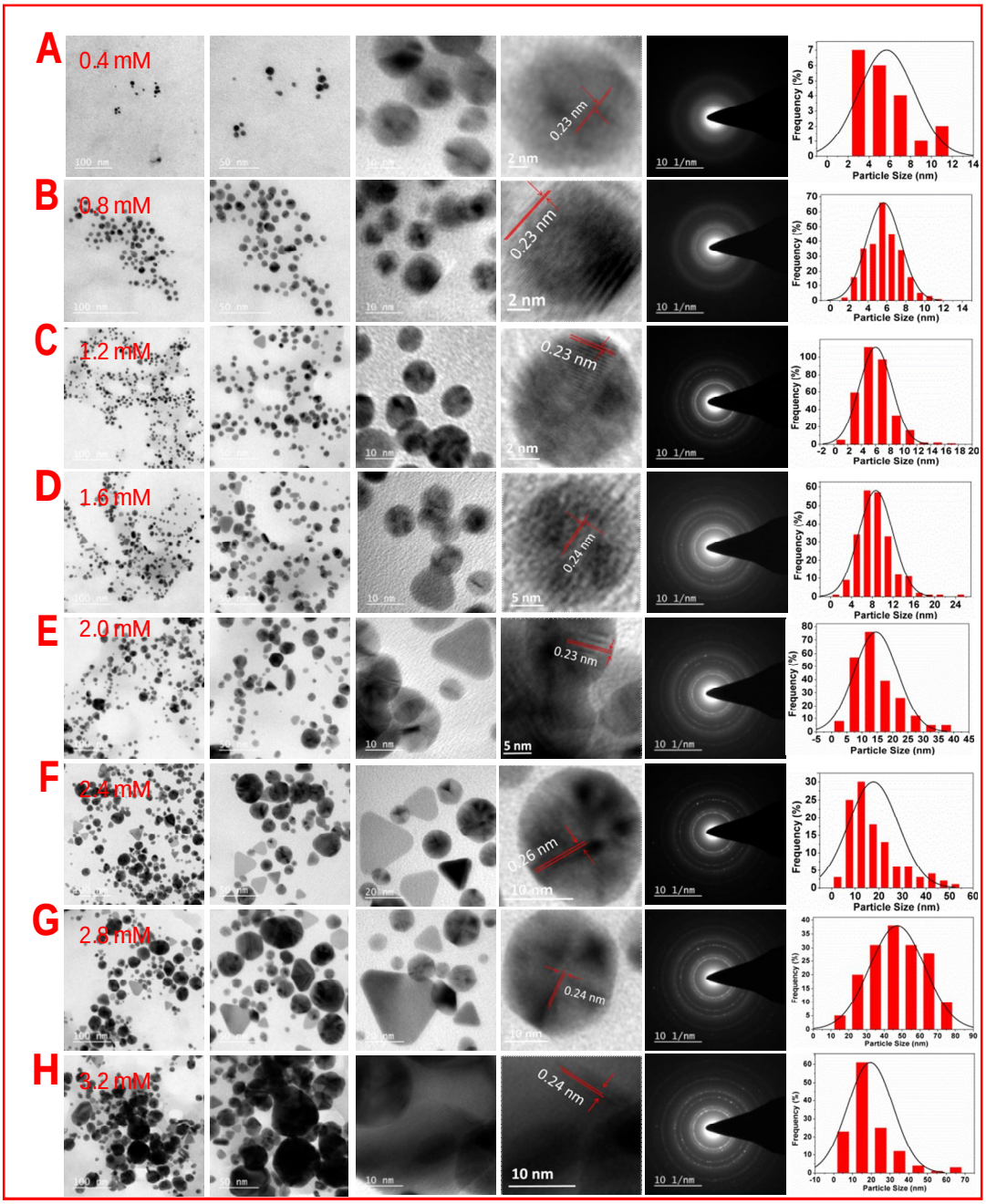

Figure 6.6 HRTEM images of AuNPs obtained from different $HAuCl_4.xH_2O$ concentration (0.4 mM to 3.2 mM) at different magnifications, their corresponding SAED pattern and histogram showing the crystalline nature of AuNPs and size distribution respectively

When the concentration was further increased by 1.2 mM, the number of spherical AuNPs thus produced also increased and observed in the range of the 1 nm to 17 nm with the average size of 6.1 nm as revealed by histogram. It was noticed that as the concentration of $HAuCl_4.xH_2O$ increased by 1.6 mM, the formation of spherical AuNPs with somewhat larger size was maintained up to this. The histogram revealed that the AuNPs were in the range of 1 nm to 19 nm with an average size 8.6 nm. Further, the TEM analysis of 2.0 mM to 3.2 mM $HAuCl_4.xH_2O$ concentrations revealed that the synthesis of anisotropic like trigonal, hexagonal AuNPs with larger size and range were increased. The anisotropic AuNPs produced from 2.0 mM, 2.4 mM, 2.8 mM, and 3.2 mM ranged from 1 nm to 37 nm, 4.5 nm to 52 nm, 6 nm to 60 nm, and 11 nm to 79 nm with an average size 13.2 nm, 14.5 nm, 17.68 nm, and 19.4 nm respectively.

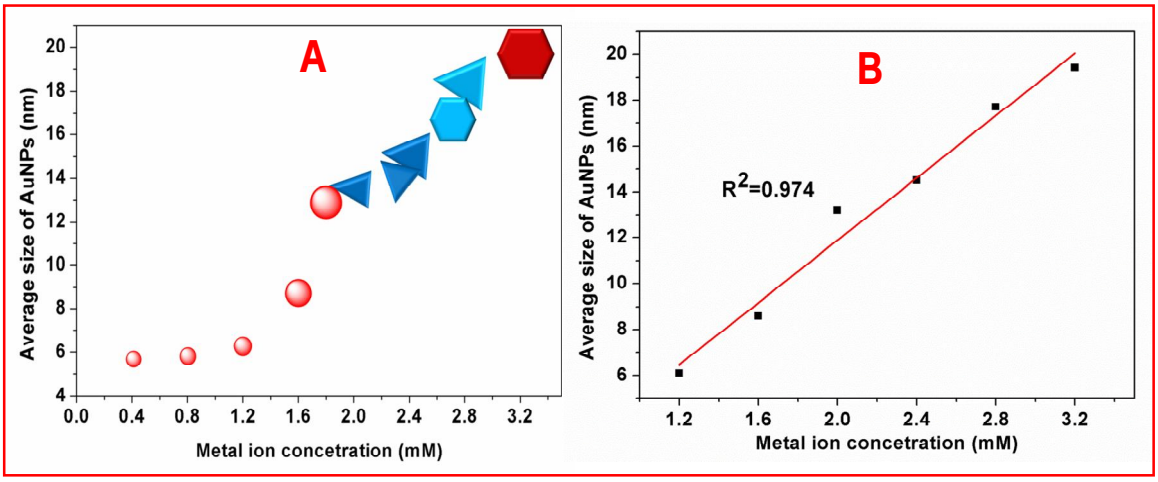

Figure 6.7 Graphical representation of change in average size and shapes of AuNPs with the increase in $HAuCl_4.xH_2O$ concentration from 0.4 mM to 3.2 mM, (B) linear relationship between the average size and corresponding $HAuCl_4.xH_2O$ concentration

In brief, it was noticed that on increasing the $HAuCl_4.xH_2O$ concentrations, the average size of the AuNPs and the synthesis of larger anisotropic AuNPs increased (**Fig.**

6.7A). The pattern of increasing average size of AuNPs corroborated a good linear relationship by increasing the $HAuCl_4.xH_2O$ concentrations having $R^2 = 0.976$ (**Fig. 6.7B)**. A close look at the SAED pattern of the 0.4 mM $HAuCl_4.xH_2O$ concentrations suggested very less circular ring which advocated the fewer number of AuNPs whereas others suggested the presence of clear circular rings advocating the crystalline nature of the AuNPs. The SAED pattern of all the AuNPs obtained from each $HAuCl_4.xH_2O$ concentrations showed the same circular ring pattern showing the crystalline nature of the AuNPs except of 0.4 mM and 0.8 mM which did not show any circular ring.

The XPS analysis was used to characterize the elemental composition of the synthesized AuNPs. The survey scan spectrum of AuNPs is shown in **Figure 6.8A.** The wide scan survey spectrum exhibited the peaks corresponding to Au 4f, C 1s, and O 1s which depicted Au, C, and O as a major element present in the sample. The peaks of C and O clearly indicated the involvement of biological moieties in the stabilization of the AuNPs. **Figure 6.8B** showed the Au 4f core level spectrum of AuNPs. The Au 4f spectrum of Au corroborated two peaks at 83.48 and 87.64 eV which corresponded to the binding energies of Au $4f_{7/2}$ and Au $4f_{5/2}$ respectively. The splitting of the 3d doublet of Au was 4.16 eV, indicating the formation of metallic AuNPs (Au^0) which indicated to the presence of pure Au (Zhou *et al*. 2010). The core level C 1s spectrum (**Fig. 6.8C)** had three Gaussian peaks at 286.9 and 288.4 eV and 289.7 eV which assigned to C–O–C/C–OH, C=O/C–Au and COOH/O–C=O respectively. **Figure 6.8D** which showed three peaks of the O 1s signal at 532.0, 533.1, 533.7 and 534.3 eV. The peak at 532.0 eV indicated the presence of, C=O whereas the peaks at 533.1 eV and 533.7 eV represented to the C–O and C–O–C. The peak observed at 534.3 eV advocated the presence of and C–OH respectively.

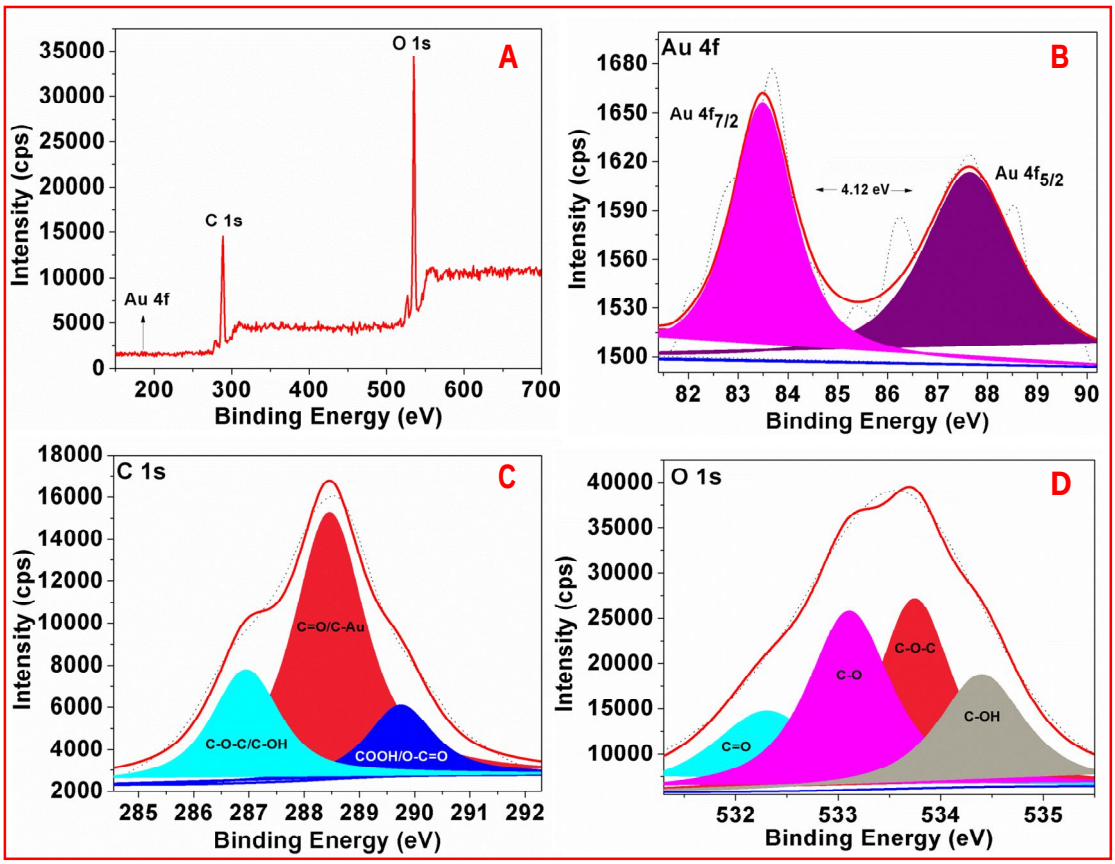

Figure 6.8 XPS spectra of AuNPs (A) wide scan spectra, (B) Au 4f spectrum, (C) C 1s spectrum (D) O 1s spectrum.

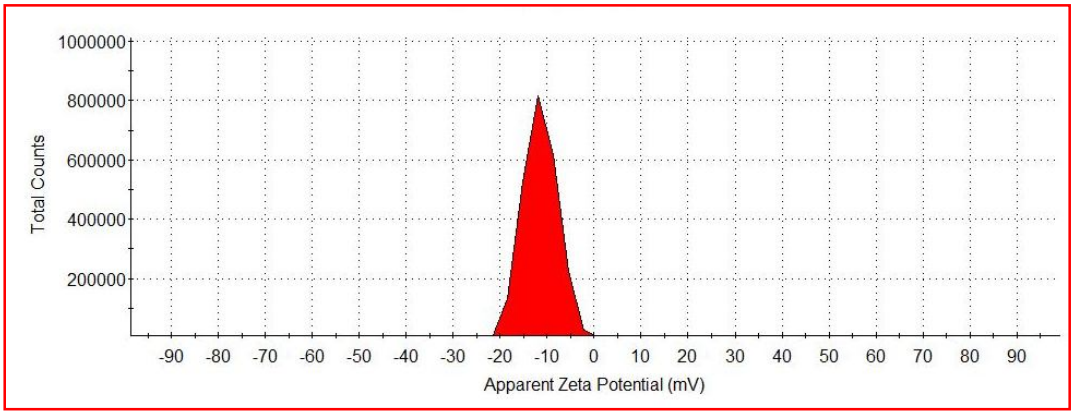

Figure 6.9 Zeta potential showing the negatively charged surface of AuNPs

The zeta potential study indicated that the surface of the AuNPs were negatively charged (-11.5) which exhibited good stability in suspension (**Fig. 6.10**).

6.6 Peroxidase-like catalytic activity of green synthesized AuNPs

The peroxidase like activity of the green synthesized AuNPs was investigated using AuNPs+TMB+H_2O_2 system where TMB was taken as an indicator which produced blue color and intense spectra at 652 nm in oxidized form (oxTMB). When AuNPs was added in to the TMB+H_2O_2 system, the color changed from colorless to blue color along with sharp spectra at 652 nm was observed. This phenomenon indicated the peroxidase like activity of the green synthesized AuNPs which catalyses the oxidation of TMB in the presence of H_2O_2 (**Scheme 6.2**). The above catalytic pathway of the oxidation of TMB can be monitored by measuring the change in absorbance at 652 nm. The addition of GSH to the AuNPs+TMB+H_2O_2 system resulted in decrease in absorbance at 652 nm and change in color from blue to light blue and thereafter almost colorless.

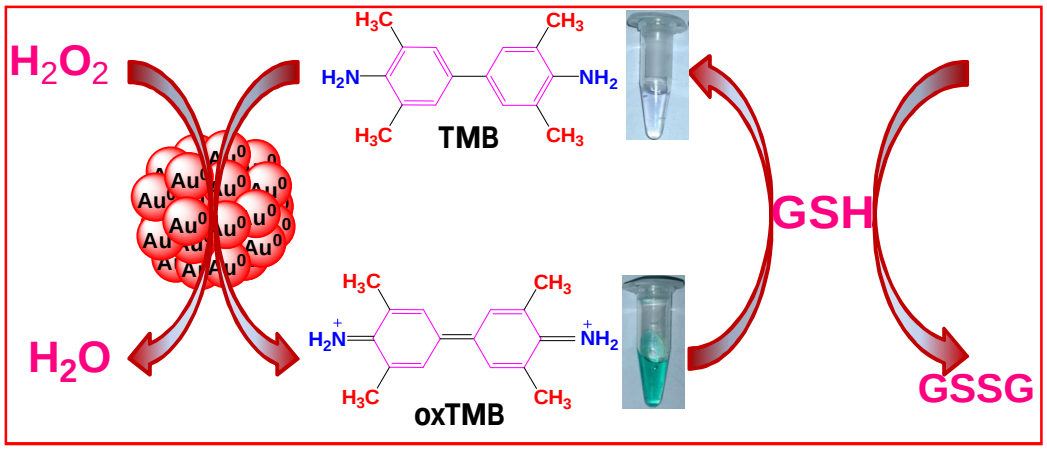

Scheme 6.2 Mechanism of peroxidase-like activity of AuNPs for the colorimetric detection of GSH

This phenomenon may be due to the reduction of the oxTMB by GSH (**Scheme 6.2**). On the basis of finding of such result, the authors are encouraged to establish a simple method for the selective and sensitive colorimetric detection of GSH.

The UV-visible absorption spectra of TMB, H_2O_2, TMB+H_2O_2, AuNPs, and AuNPs+TMB+H_2O_2 and their respective color are presented in **Figure 6.10A.** It was observed that AuNPs produced the spectrum at 542 nm whereas TMB, H_2O_2, TMB+H_2O_2 neither produced any spectra nor any color. However, when AuNPs was added in TMB+H_2O_2, an intense spectra at 652 nm with blue color was produced which indicated that green synthesized AuNPs can be used for the catalytic oxidation of TMB to oxTMB. Whereas when GSH was added in to the AuNPs+TMB+H_2O_2, the blue color disappeared and the absorbance of the spectra decreased (**Figure 6.10B**).

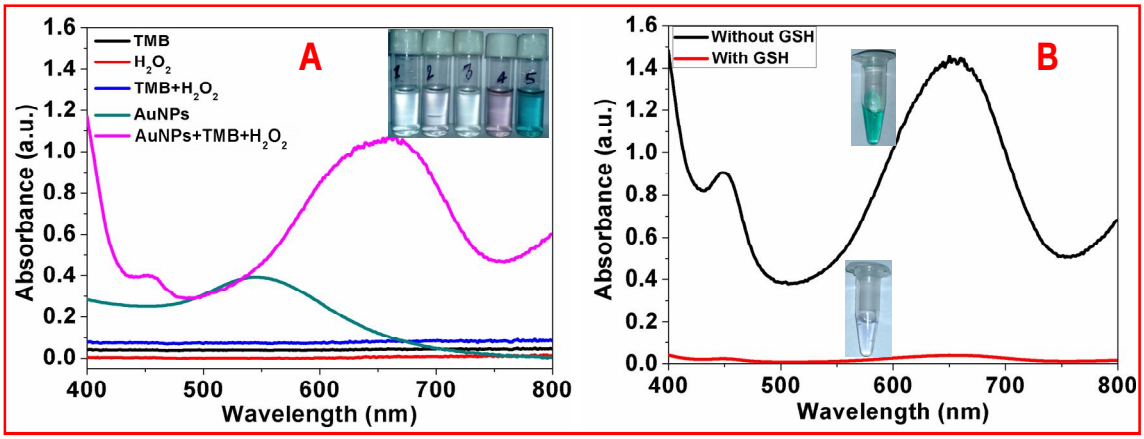

Figure 6.10 UV-visible absorbance spectra of (A) TMB, H_2O_2, TMB+H_2O_2, AuNPs, AuNPs+TMB+H_2O_2, and (B) AuNPs+TMB+H_2O_2 solution in the presence and absence of GSH and their corresponding digital images

6.6.1 Optimization of factors affecting peroxidase-like activity

The various factors affecting the peroxidase-like activity of AuNPs such as incubation time, pH, temp, TMB concentration, H_2O_2 concentration, AuNPs concentrations were optimized using one parameter at a time approach for obtaining the optimum result for the better performance against the detection of glutathione.

Figure 6.11A showed the peroxidase like activity of AuNPs at different pHs in the range of 1-10. It was observed that AuNPs exhibited excellent peroxidase like activity at pH 4. As the pH increased beyond 4 the peroxidase like activity of AuNPs started to decrease towards higher pH due to decomposition of H_2O_2 into H_2O and O_2 rather $OH^{\bullet}$ radical (Feng *et al*. 2017). Therefore, pH 4 was considered as optimum pH for better peroxidase like activity of AuNPs. Thereafter, the effect of temperature on the peroxidase like activity of AuNPs was also optimized at constant pH 4.

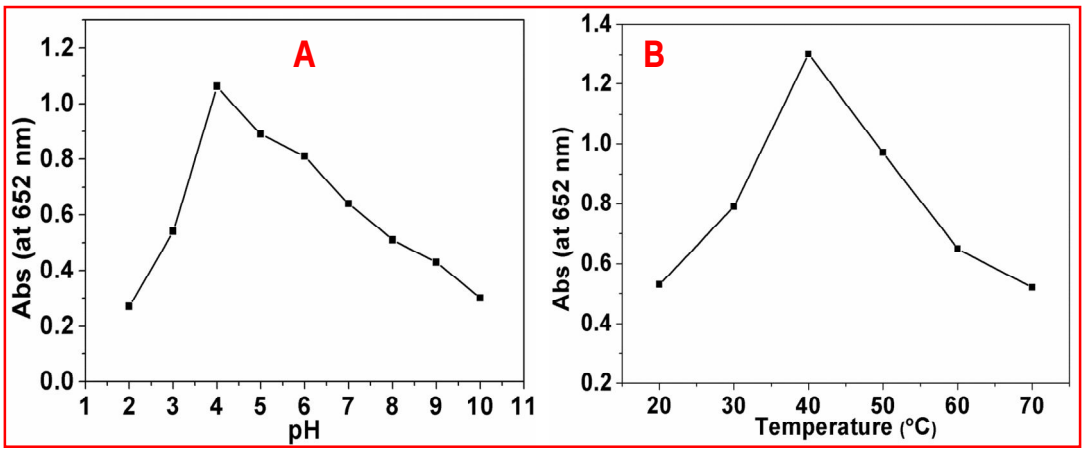

Figure 6.11 Peroxidase-like activity of AuNPs at different (A) pHs (2 – 10) at 37 ^{o}C, and (B) temperatures, (20 – 70 ^{o}C) at pH 4 using AuNPs (50 µL) + TMB (50 µL, 1 mM) + H_2O_2 (50 µL, 1 mM) in 200 µL of 0.2 M NaAc buffer solution

Figure 6.11B showed the optimum peroxidase like activity at temperature 40 ^{o}C. Further, on increasing the temperature, the peroxidase like activity decreased due to agglomeration of AuNPs which led to the hindrance of electron transfer (Feng *et al*. 2017).

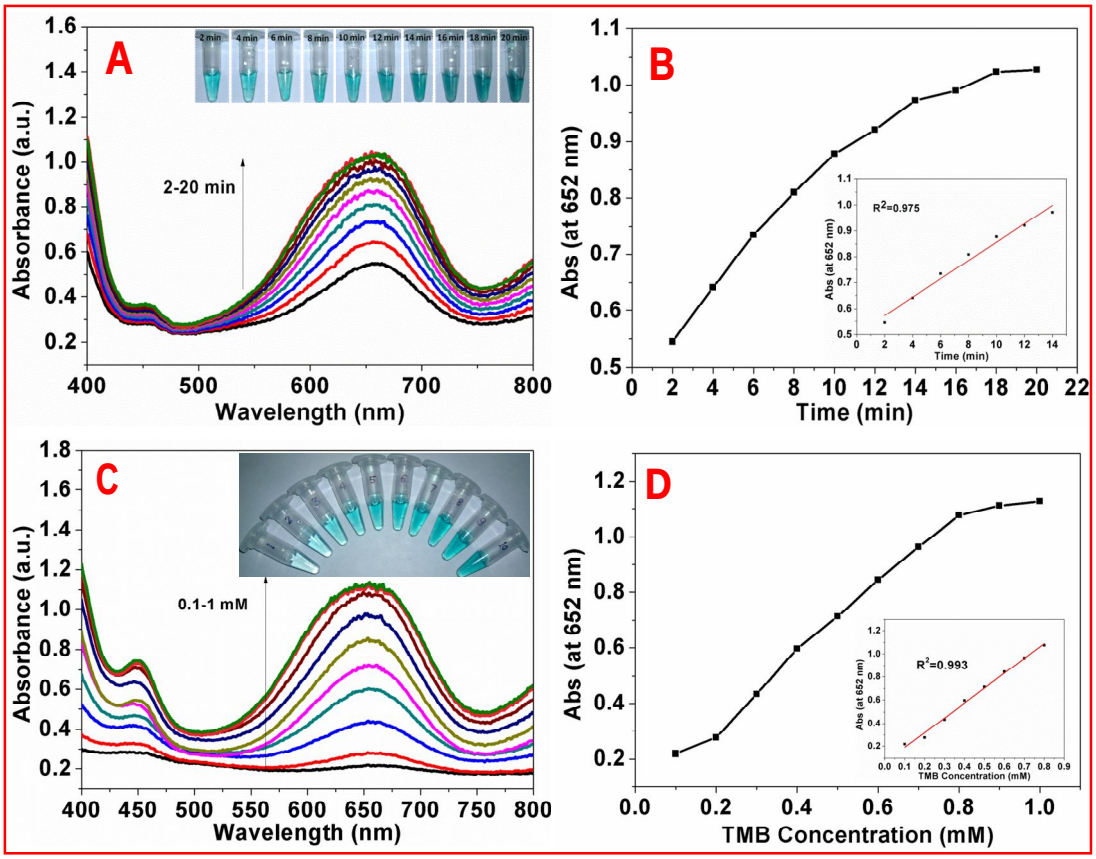

Figure 6.12 Peroxidase like activity of AuNPs at pH 4 and temp 40 ^{o}C at (A) different time interval from 2 to 20 min using 50 µL of 1 mM TMB, 50 µL of 1 mM H_2O_2 and 50 µL of AuNPs in 200 µL of NaAc buffer with inset photographs of corresponding change in color, (B) relationship between absorbance and incubation time with inset calibration plot showing the linear relationship between 2 to 14 min with R^2 = 0.995, (C) different concentrations of TMB at pH 4 and temp 40 ^{o}C using 50 µL (1 mM) H_2O_2 and 50 µL of AuNPs in 200 µL of NaAc buffer at 18 min of fixed incubation time with inset photographs of corresponding change in color, (D) relationship between absorbance and TMB concentrations with inset calibration plot showing the linear relationship between 0.1 to 0.8 mM with R^2 = 0.993

For optimizing the incubation time required for obtaining the maximum absorbance at 652 nm, the samples were screened and UV-visible spectra were recorded simultaneously. **Figure 6.12A** showed the absorption spectra of the reaction system at 652 nm at different time interval. The darkening of the color from light blue to dark blue and intensity of the spectra were observed to be increased on increasing the incubation time only upto 18 min and thereafter no significant change was observed. Therefore, 18 min of incubation time was chosen as optimum time. The calibration plot of increase in absorbance vs incubation time showed a good linear relationship in the range of 2-14 min with R^2 = 0.975 (**Fig. 6.12B**). Similarly, the effect of different concentration of TMB, AuNPs amount and H_2O_2 concentration was optimized at 18 min of incubation time, pH 4, and temp 40 ºC. It was observed that initially, the peroxidase like activity increased upto an optimum value. Thereafter, no significant change in absorbance was observed.

Figure 6.12C and **D** represented the optimum TMB concentration was 0.8 mM using 50 µL H_2O_2 (1 mM) and 50 µL AuNPs having linear relationship between 0.1 mM to 0.8 mM with R^2 = 0.993. **Figure 6.13A** and **B** showed that the optimum AuNPs amount was 80 µL using 50 µL H_2O_2 (1 mM) and 50 µL TMB (0.8 mM) having linear relationship between 10 µL to 60 µL AuNPs with R^2 = 0.976. The optimum activity of H_2O_2 was observed at 8 mM using 80 µL AuNPs and 50 µL TMB (0.8 mM) having linear relationship between 2 mM to 8 mM with R^2 = 0.997 (**Fig. 6.13C and D**). Beyond these optimum concentrations no significant change in absorbance was observed because of over concentration which increased the agglomeration of AuNPs.

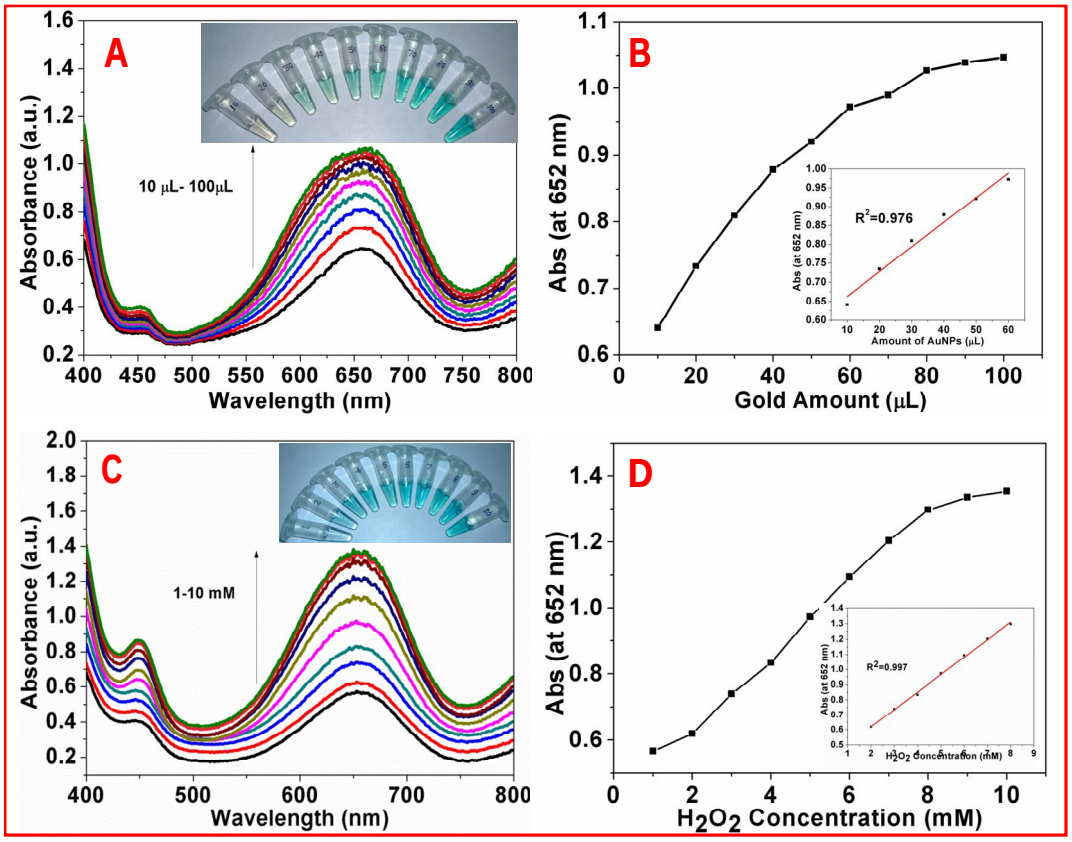

Figure 6.13 Peroxidase-like activity of AuNPs at pH 4 and temp 40 ^{o}C at (A) different amount of AuNPs using 50 µL (1 mM) H_2O_2 at constant 18 min of incubation time and 50 µL of 0.8 mM TMB with inset photographs of corresponding change in color, (B) relationship between absorbance and AuNPs amount with inset calibration plot showing the linear relationship between 0.1 to 0.8 mM with R^2 = 0.993, (C) different concentrations of H_2O_2 using at constant 18 min of incubation time 50 µL of 0.8 mM TMB and 80 µL of AuNPs with inset photographs of corresponding change in color, (D) relationship between absorbance and AuNPs amount with inset calibration plot showing the linear relationship between 0.1 - 0.8 mM with R^2 = 0.997

6.6.2 Detection of GSH

The sensing potential of the proposed AuNPs+TMB+H_2O_2 system towards the detection of GSH was observed by change in color of the system from blue color to colorless which can be seen by naked eye **(Fig. 6.10B)**. It was observed that as the concentration of the

GSH increased from 1.0 to 120 µM, the color of the AuNPs+TMB+H_2O_2 system turned dark blue to light blue due to the continued reduction of oxTMB into reduced form (**Fig. 6.14A**).

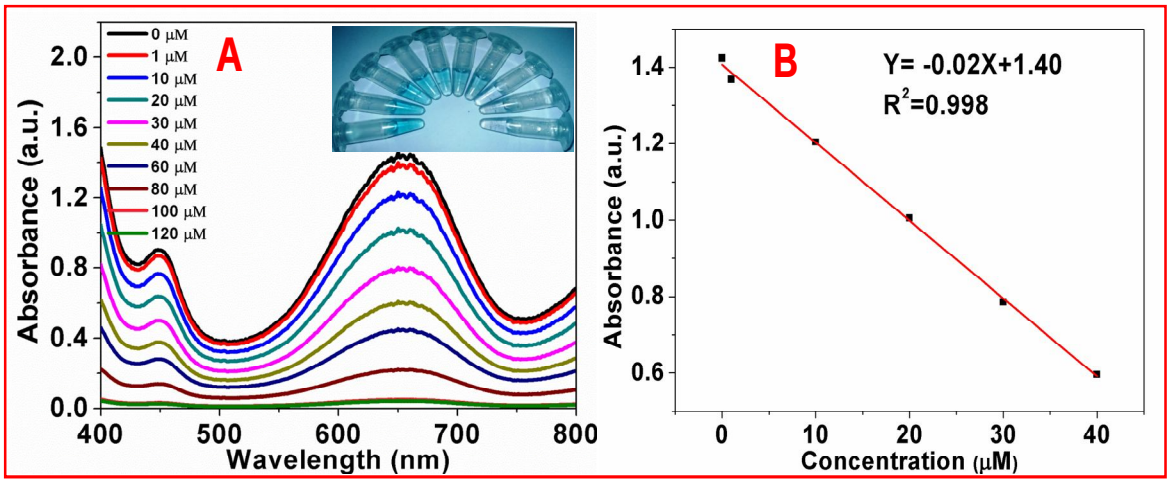

Figure 6.14 (A) UV-visible spectra of AuNPs+TMB+H_2O_2 system showing sensitive detection of GSH in the absence and presence of its different concentrations with inset photographs showing the corresponding change in color from dark blue to almost transparent with the increasing GSH concentrations, (B) relationship between absorbance and GSH concentrations showing the linear relationship between 1 - 40 µM with R^2 = 0.998

Figure 6.14A revealed that no change in absorption at 652 nm and color was observed in the reaction system without GSH. **Inset Figure 6.14A** clearly corroborated the gradual decrease in color intensity on increasing the GSH concentration up to 120 µM. It was also observed that when the concentration of the GSH increased from 0.1 to 120 µM, the absorbance at 652 nm decreased gradually due to the reduction of oxTMB (Ni *et al*. 2015) . It can be concluded that the green synthesized AuNPs can be used as a green catalyst for the oxidation of TMB which can be used for the colorimetric detection of GSH. **Figure 6.14B** revealed a good linear relationship between absorbance and different concentration of the GSH from 0.1 µM to 40 µM with high value of R^2 (0.998). The limit of the detection (LOD)

was calculated to be 0.013 µM which was excellent than previously reported works (**Table 6.2**).

Table 6.2 Different sensors developed for the detection of GSH

Probe	Mode	Linear Range	Detection limit	Detection time	References
MnO_2 NPs-TMB	Colorimetry	0.26-26 µM	0.1 µM	15 min	Liu *et al*. 2013
AuNPs-ppzdtc	Colorimetry	8-250 nM	8 nM	30	Li *et al*. 2011
CQDs-AuNPs	Colorimetry	1.0-4.0 µM	-	5 min	Shi *et al*. 2014
Fe_3O_4-ABTS-H_2O_2	Colorimetry	3.0-30 µM	-	20	Ma *et al*. 2012
SAMb-AuNPs	Colorimetry	0.2-0.9 µM	21.7 nm	-	Zhi-Jian 2015
PEI–capped AgNCs	Fluorometry	0.5-0.6 µM	38 µM	30 min	Zhang *et al*. 2013
EDC/CQDs fluorescence	Fluorometry	1.0–50 µM	0.943 µM	10 min	Li Yan 2017
AuNPs	Colorimetry	0.1-40 µM	0.013 µM		Present Work

The selectivity towards the colorimetric detection of GSH was examined by adding 50 µL (100 µM) of each Gly, Val, Ala, Leu, Ile, Phe, Ser, Thr, Tyr, Met, His, Asp, Glu, Trp, Lys, Arg, Asn, Pro, Csy, and GSH into the TMB+H_2O_2+AuNPs system. **Figure 6.15** showed the ΔA of TMB+H_2O_2+AuNPs system at 652 nm after introduction of GSH and various other amino acids. It was observed that ΔA of GSH was surprisingly larger than others. A little change in absorbance (ΔA) was observed with the Met and Csy which were negligible as compared to previously reported literatures (Zhang *et al*. 2013, Tang *et al*. 2013). Thus it was concluded that the developed sensor system showed good selectivity in the presence of others thiol containing amino acids.

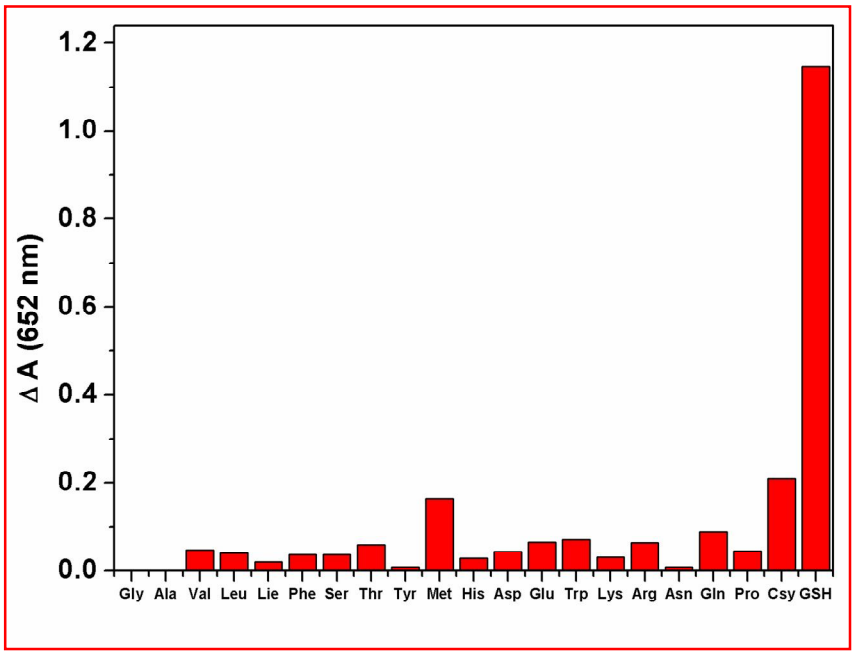

Figure 6.15 Selectivity of the TMB+H_2O_2+AuNPs system for the detection of GSH

6.6.3 Detection of GSH in real samples

High selectivity and sensitivity of the AuNPs+TMB+H_2O_2 system towards the detection of GSH encouraged us to detect the GSH in real samples. Hence; the utility of the AuNPs+TMB+H_2O_2 system was examined for the detection of GSH in human blood serum obtained from Sir Sundarlal Hospital, Banaras Hindu University, Varanasi, U.P., India, 221005. For this, the human serum samples were diluted and spiked with the known amount of GSH. **Figure 6.16A** and **B** showed the UV-visible spectra and bar diagram of serum samples at 652 nm. The spectra and bar diagram and **Inset Figure 6.16B** indicated that serum 1 having highest concentration whereas serum 4 having lowest concentration of GSH. The recovery of the GSH was calculated and given in **Table 6.3.** The recovered amount of

GSH was in the range of 96.3% to 108.2%. Such a high recovery advocated that the AuNPs+TMB+H_2O_2 system is applicable and reliable for the real clinical samples analysis.

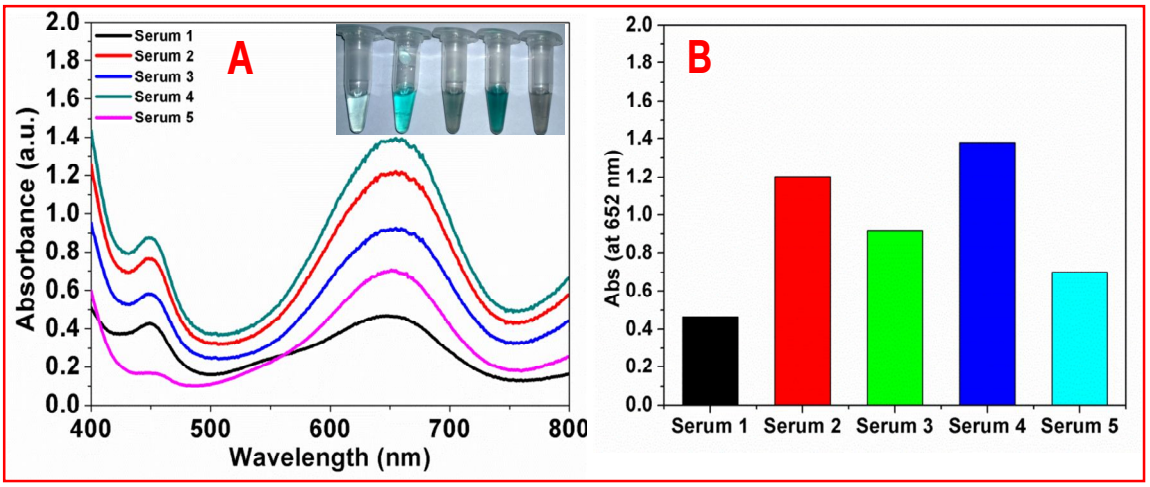

Figure 6.16 (A) Detection of GSH in serum samples with inset photographs showing the respective color change and (B) their corresponding bar diagram

Table 6.3 Utilization of the developed sensor system for the detection of GSH in real samples

Sample	Without Spiking (μM)	GSH Spiked (μM)	GSH Measured (μM)	Recovery (%)
Serum 1	18.84	5	24.25	108.2
Serum 2	8.50	10	18.00	95.0
Serum 3	12.85	15	27.30	96.3
Serum 4	0.69	20	20.35	98.3
Serum 5	9.66	25	35.35	102.8

6.7 Conclusion

An attempt has been made to develop completely eco-friendly and economically viable route for the green synthesis of AuNPs. For this, AEC was used as a potent reducing and stabilizing agent photoinduced route was adopted as it avoided the need of heating and stirring. The parameters affecting the synthesis process were optimized using one parameter

at a time approach and observed that 24 min of sunlight exposure time, 4% AEC inoculums dose and 1.6 mM $HAuCl_4.xH_2O$ concentration were the optimum parameters. The comparative study of FTIR analysis of AEC with pure tannic acid effectively confirmed the involvement of polyphenolics which were already reported and also confirmed by our group; in the synthesis and stabilization of AuNPs. The XRD analysis confirmed the synthesis of pure metallic gold with FCC lattice. The TEM images revealed the increase in average size and anisotropy with the increase in $HAuCl_4.xH_2O$ concentration. The presence of two individual peaks attributing to the binding energies of Au $4f_{7/2}$ and Au $4f_{5/2}$ in XPS analysis again strengthened the fact of presence of metallic gold. The AuNPs thus obtained showed as a peoxidase-like mimicking acitivity which catalyzed the oxidation of TMB to oxTMB with the development of blue color and absorption spectra at 652 nm. However, the presence of GSH caused further reduction of oxTMB. This detection experiment showed good linear relationship between 1 µM to 40 µM with the limit of detection 0.013 µM. In addition to this, the greater recovery of GSH from human blood serum advocated that the developed system was simple and sensitive for the real sample analysis.